

MICROCOPY RESOLUTION TEST CHART
NATIONAL BUREAU OF STANDARDS 1963-A

12

AD



US ARMY
MATERIEL
COMMAND

TECHNICAL REPORT BRL-TR-2701

AD-A163 919

CONVECTIVE HEATING OF
ENERGETIC MATERIALS

Richard A. Beyer
Mark A. DeWilde

December 1985

DTIC
ELECTE
JAN 31 1986
S D
D

APPROVED FOR PUBLIC RELEASE; DISTRIBUTION UNLIMITED.

US ARMY BALLISTIC RESEARCH LABORATORY
ABERDEEN PROVING GROUND, MARYLAND

DTIC FILE COPY

Destroy this report when it is no longer needed.
Do not return it to the originator.

Additional copies of this report may be obtained
from the National Technical Information Service,
U. S. Department of Commerce, Springfield, Virginia
22161.

The findings in this report are not to be construed as an official
Department of the Army position, unless so designated by other
authorized documents.

The use of trade names or manufacturers' names in this report
does not constitute indorsement of any commercial product.

UNCLASSIFIED

SECURITY CLASSIFICATION OF THIS PAGE (When Data Entered)

REPORT DOCUMENTATION PAGE		READ INSTRUCTIONS BEFORE COMPLETING FORM	
1. REPORT NUMBER Technical Report BRL-TR-2701	2. GOVT ACCESSION NO. AD-A163919	3. RECIPIENT'S CATALOG NUMBER	
4. TITLE (and Subtitle) CONVECTIVE HEATING OF ENERGETIC MATERIALS		5. TYPE OF REPORT & PERIOD COVERED Final	
		6. PERFORMING ORG. REPORT NUMBER	
7. AUTHOR(s) Richard A. Beyer Mark A. DeWilde		8. CONTRACT OR GRANT NUMBER(s)	
9. PERFORMING ORGANIZATION NAME AND ADDRESS US Army Ballistic Research Laboratory ATTN: SLCBR-IB Aberdeen Proving Ground, MD 21005-5066		10. PROGRAM ELEMENT PROJECT, TASK AREA & WORK UNIT NUMBERS 1L161102AH43	
11. CONTROLLING OFFICE NAME AND ADDRESS U.S. Army Ballistic Research Laboratory ATTN: SLCBR-DD-T Aberdeen Proving Ground, MD 21005-5066		12. REPORT DATE December 1985	
		13. NUMBER OF PAGES 27	
14. MONITORING AGENCY NAME & ADDRESS (if different from Controlling Office)		15. SECURITY CLASS. (of this report) UNCLASSIFIED	
		15a. DECLASSIFICATION/DOWNGRADING SCHEDULE N/A	
16. DISTRIBUTION STATEMENT (of this Report) Approved for Public Release; Distribution Unlimited			
17. DISTRIBUTION STATEMENT (of the abstract entered in Block 20, if different from Report)			
18. SUPPLEMENTARY NOTES			
19. KEY WORDS (Continue on reverse side if necessary and identify by block number) HMX Fluorescence RDX NOSOL 363 Pyrolysis Ignition Shadowgraph			
20. ABSTRACT (Continue on reverse side if necessary and identify by block number) meg The pyrolysis and ignition dynamics of propellants and their components have been explored using convective heating at a flow rate of about 1 m/s at atmospheric pressure. Two major techniques were used for the dynamics studies. The first was a video camera and recorder which were used to record flame luminescence. Also used to study ignition dynamics was a high-speed shadow photography system which characterized regions of heat release following immersion of single propellant grains in the hot flow. A key			

DD FORM 1 JAN 73 1473 EDITION OF 7 NOV 65 IS OBSOLETE

UNCLASSIFIED

SECURITY CLASSIFICATION OF THIS PAGE (When Data Entered)

COPY

UNCLASSIFIED

SECURITY CLASSIFICATION OF THIS PAGE(When Data Entered)

20. Abstract (Cont'd):

observation was an unusual two-stage flame observed with NOSOL 363; no previous report has shown similar behavior with this propellant.

Gas released during pyrolysis was analyzed using grab samples and infrared absorption spectroscopy. Key observations with HMX were (a) the increase in relative amount of NO_2 with respect to other species with increasing temperature, and (b) the probable detection of substantial amounts of formic acid. This latter has not previously been observed in HMX pyrolysis studies.

Fluorescence imaging techniques were evaluated and demonstrated to have sufficient sensitivity for dynamic ignition studies.

UNCLASSIFIED

SECURITY CLASSIFICATION OF THIS PAGE(When Data Entered)

11

TABLE OF CONTENTS

	<u>Page</u>
LIST OF FIGURES.....	5
I. INTRODUCTION.....	7
II. DESCRIPTION OF EXPERIMENT.....	7
III. OBSERVATIONS.....	9
A. Dynamics.....	9
B. Evolved Gas Analysis.....	12
C. Planar Fluorescence.....	14
IV. DISCUSSION/ANALYSIS.....	14
SUMMARY.....	18
ACKNOWLEDGEMENTS.....	19
REFERENCES.....	20
DISTRIBUTION LIST.....	21

Accession For	
NTIS CRA&I	<input checked="" type="checkbox"/>
DTIC TAB	<input type="checkbox"/>
Unannounced	<input type="checkbox"/>
Justification	
By	
Distribution/	
Availability Codes	
Dist	Avail. and/or Special
A-1	



LIST OF FIGURES

<u>Figure</u>		<u>Page</u>
1	Schematic Diagram of Shadowgraph/Pyrolysis Apparatus.....	8
2	Schematic of the Planar Laser Fluorescence Apparatus.....	9
3	Shadowgraphs of NOSOL 363 Propellant Grain in Flow of Air at Four Times, Showing (a) The Flame Front, (b) The Wire Holder, (c) Pieces of Burning Propellant, and (d) Heat Release Near Surface of Grain. Zero time is entry of grain into the hot flow.....	11
4	Infrared Absorption Spectrum of Gases Collected in the Wake of M30 Propellant Grain Pyrolyzed by Flow of 390°C Nitrogen.....	12
5	Infrared Absorption Spectrum of Gases Collected in the Wake of HMX Pellet Pyrolyzed by Flow of (a) 560°C and (b) 390°C Nitrogen.....	13
6	Infrared Absorption Spectrum of Gases From Pyrolysis of RDX/HTPB by 360°C Nitrogen.....	14
7	The Ratios of Four Major Species to N ₂ O at a Constant Flow Velocity Near 1 m/s as a Function of the Nitrogen Temperature at the Position of the Grain.....	17

PREVIOUS PAGE IS BLANK

I. INTRODUCTION

The role of gas-phase chemistry in the ignition of gun propellants is not a well understood phenomenon. In particular, previous studies¹ with a large-caliber gun simulator have shown that with base pad-only ignition a cloud of gases forms and ignites after a delay period; ignition of the solid propellant follows shortly thereafter. Although these tests are deliberately extreme examples, they are essential to understanding the processes which can take place during both normal and anomalous ignition cycles. In particular, the further characterization of these ignition processes and exploitation of this understanding requires information about convective pyrolysis of propellant grains, the amount of heat release during pyrolysis, and the details of the controlling processes during the onset of ignition in the gas phase near the propellant grain. In this paper we describe qualitative experiments to show the flow field and heat generation from single propellant grains during and convectively supported burning of propellant grains in laminar flows of hot gases. We also report some gas compositions in the wake of convectively pyrolyzed samples of propellants and related materials. Preliminary planar laser fluorescence studies of NO_2 in the wake of pre-ignition RDX/HTPB binder propellants have been performed to define the sensitivity and requirements of this technique for ignition dynamic studies.

II. DESCRIPTION OF EXPERIMENT

A schematic diagram of the main apparatus is shown in Figure 1. The source of hot gas for these studies is a compact electric heat exchanger constructed from stainless steel flow channels and furnace heating elements. Flow channels are nominal 9.5 mm i.d. Power requirement for the heating elements is 25A at 110V. After preheating the flow channels for approximately two hours, flows in excess of 900°C with velocities on the order of 1 m/s have been obtained with laminar, uniform flow. A series of screens is used in the flow immediately before exit to provide a uniform velocity profile as measured with a 1.6 mm diameter pitot tube. Both air and nitrogen have been used in these studies as the flow gas. For most of the shadowgraph studies reported here, the samples were injected into the established flow with an air driven piston which was triggered by the camera when necessary. A water-cooled shutter was used for pyrolysis studies so that the samples could be pre-positioned with respect to the gas sampling tube.

Flow and heat release observations have been made in two manners. The first was to use a standard video camera and recorder and later a high speed (12,000 frames/s) camera to record the light emission from ignition or combustion of the sample. The second method, shown in Figure 1, was to use a 100 mW argon ion laser to generate shadowgraphs which were filmed at 12,000 frames/s. The laser beam diameter was 100 mm in the sample region; a 1.22 m focal length schlieren grade mirror imaged the light onto the film.

¹T.C. Minor, "Characterization of Ignition Systems for Bagged Artillery Charges," Proceedings of 17th JANNAF Combustion Meeting, CPIA Publication No. 329, Vol. II, p. 45, 1980.

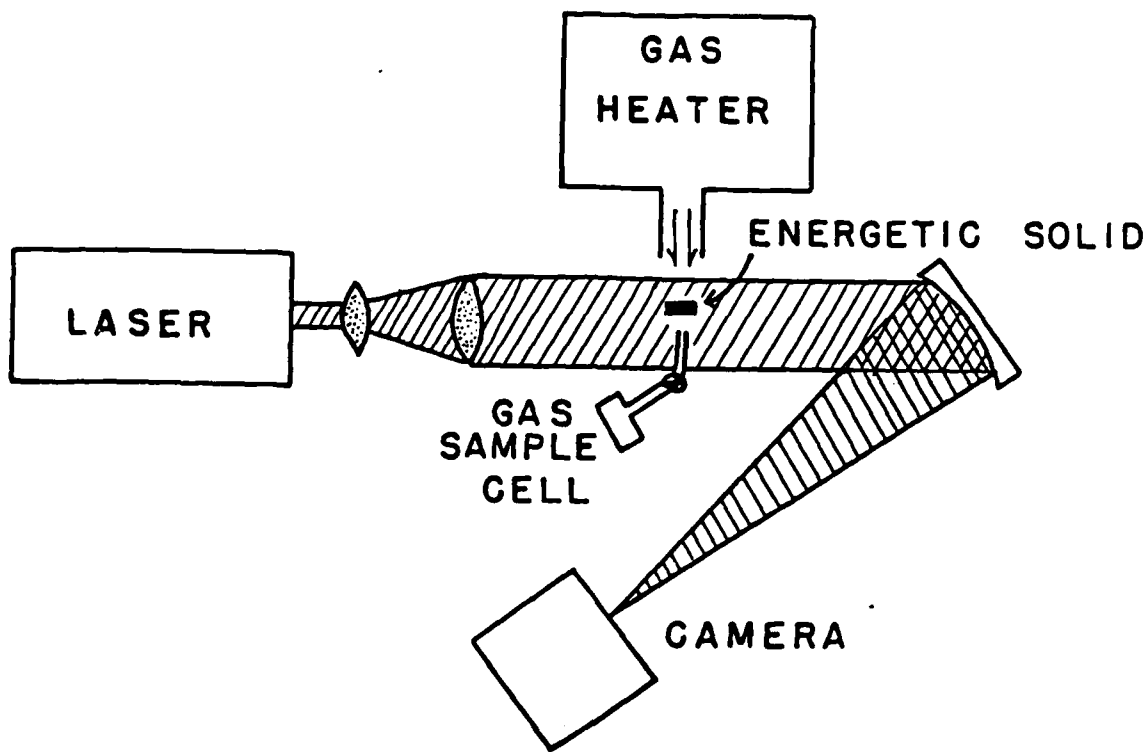


Figure 1. Schematic Diagram of Shadowgraph/Pyrolysis Apparatus

Pyrolysis gas products were measured by taking samples from the wake of a pyrolyzing solid into a 100 cm^3 evacuated cell. These gases were then analyzed by conventional infrared absorption spectroscopy to determine the major stable species.

Three principal sample types were used. The first was standard seven perforation grains of M30 propellant, 4 mm in diameter and 10 mm long. The second sample type was NOSOL 363 in single perforation grains cut in 10 mm lengths from 8 mm diameter stick propellant.² The HMX decomposition was studied with pellets pressed from 100 mg of 150 to 300 μm crystals with typical dimensions of 6 mm in diameter and 2 mm thick. Observations were also made with RDX in an HTPB binder; typical samples were 3 mm thick slices from 8 mm diameter 7-perf grains.

A limited number of observations were made using the planar laser-induced fluorescence technique. A schematic diagram of this approach is shown in

²S.E. Mitchell, "Selected Properties of Navy Gun Propellants," IHSP, pp. 76-128, 1976.

Figure 2. The basic idea is to expand the laser beam in one direction to make a "sheet of light." The fluorescence is observed normal to the plane of the laser light. The result is an image of a slice through the event which is species specific and independent of edge effects. For these experiments, the laser used was a nominal 8 watt argon ion laser. The beam was expanded to approximately 40 mm (1.5 in) thick at the propellant grain. Two configurations were tried: two watts of 488 nm light with detection of all light red of 500 nm or seven watts multi-line (dominated by 488 and 514.5 nm) with detection of yellow-green light with an OG 530 filter. Detectors were a high speed camera with ASA 400 film and a 35 mm camera with an f/2.6 lens system and ASA 1000 film. For all of these tests, the samples were RDX/HTPB pyrolyzed in air at temperatures sufficiently high to cause ignition after pyrolyzing a good fraction of the sample.

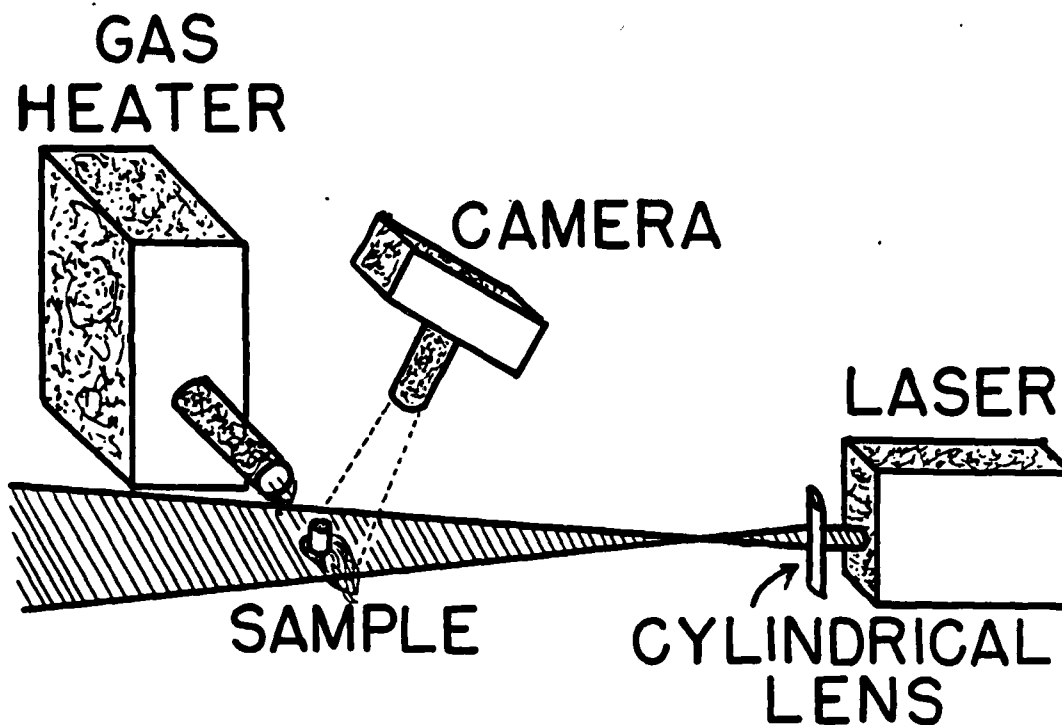


Figure 2. Schematic of the Planar Laser Fluorescence Apparatus

III. OBSERVATIONS

A. Dynamics

The first measurements were made using the video camera and recorder to record the naturally occurring luminosity from the ignition/combustion processes. The limited sensitivity of this camera yielded information only under conditions where a flow of air was used and temperatures were sufficiently high to achieve full ignition (typically above 700°C and

1 m/s). Of particular note was the observation that with grains of M30 propellant in a flow of air the first luminosity was frequently downstream from the grain and appeared to start at a point where the air and propellant wake gases might well have mixed. This downstream origin of luminosity (and probably ignition) was not observed on every sample due to the limited framing rate of the video camera; in many cases the sample went from no light detected to full combustion between frames. Ignition of the solid appeared to proceed immediately following gas phase ignition in all cases where separate initial gas phase luminosity was observed.

Using a flow of hot nitrogen under the same conditions, the luminosity was greatly reduced. Although there was sufficient luminosity to see the propellant flame once ignition was complete, the emission levels were insufficient to determine the point of ignition. Similar studies made using the high speed camera at 12,000 frames/s and ASA 400 film yielded no further information.

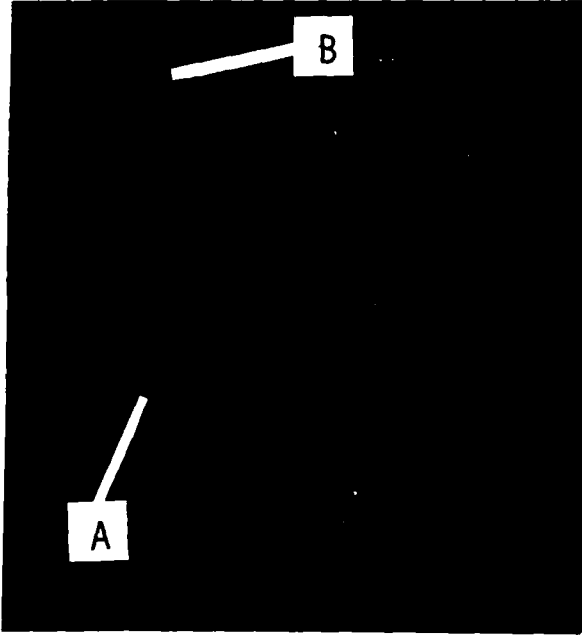
Flows and heat generation were studied further using the high speed shadowgraph system to record thermal gradients in the flow field. Although this technique was not optimized to the point where the point of ignition could be determined, qualitative observations have been made with M30 and NOSOL 363 propellant grains. Typical conditions for these observations were a flow of 730°C nitrogen or air at about 1 m/s.

Of particular note with the M30 grains in nitrogen was the generation of substantial amounts of gas from the solid surface, beginning at least as soon as the sample reached its equilibrium position in the gas flow, typically 20 msec. Earlier evolution of gas is possible but would not be detected here because of the disturbance of the flow during injection of the sample. In addition to the surface evolution of gas, the flow of significant quantities of hot gas from the grain perforations was also recorded from the earliest times.

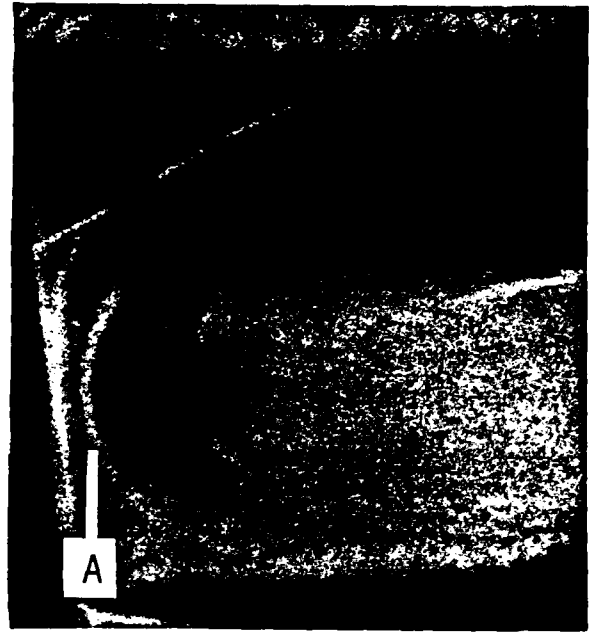
With the double base propellant grains in nitrogen, the flow field was much as anticipated with a flame (region of heat generation) swept downstream symmetrically from the leading edge of the cylindrical grain with a turbulent wake. No burning chunks were seen leaving the M30 grain until very near consumption of the grain. With a flow of air, the M30 grain observations were apparently unchanged compared to nitrogen flow.

The most dramatic events were recorded with the NOSOL 363 in a flow of air. Figure 3 shows shadowgraphs at four times during an event. In these pictures, the flow is from left to right. The gas evolution was so great during combustion that flame standoff was several millimeters upstream from the grain and the plume pushed the boundaries of the hot flow out substantially. Also obvious are the chunks of burning propellant which break off and flow away from the grain, moving both downstream and normal to the flow direction.

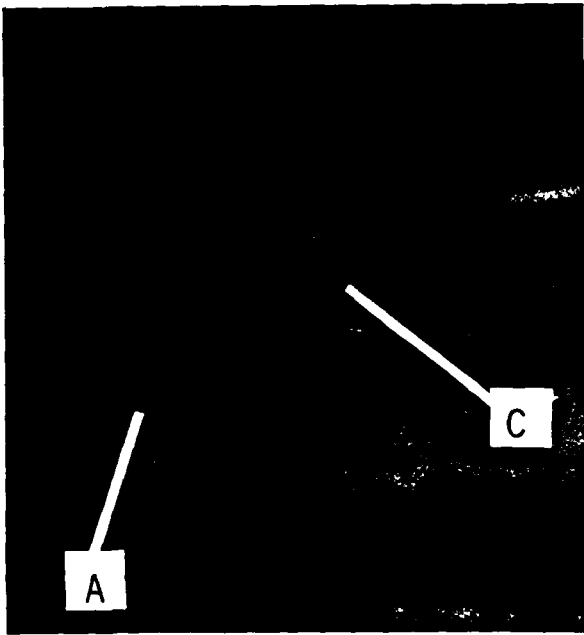
A further observation which is more apparent in viewing the films, but which can be seen in Figure 3, is the movement with time of the crescent-shaped flame front upstream from the propellant. At the first time shown this flame is apparently attached to the grain. In the second two frames it is



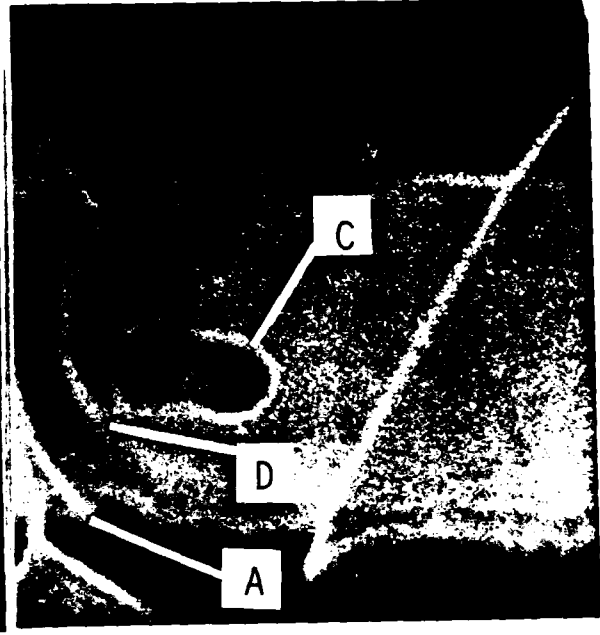
T = 300 msec



T = 460 msec



T = 640 msec



T = 800 msec

Figure 3. Shadowgraphs of NOSOL 363 Propellant Grain in Flow of Air at Four Times, Showing (a) The Flame Front, (b) The Wire Holder, (c) Pieces of Burning Propellant, and (d) Heat Release Near Surface of Grain. Zero time is entry of grain into the hot flow.

seen to move upstream away from the grain, in the fourth frame the original front has moved upstream 5 mm or more and is partially obscured; a second "flame" has by this time appeared near the grain surface. When viewed by the naked eye these two stages of heat release were not apparent. However, the total luminosity was so great under these conditions that the outer flame easily could mask that nearer the solid surface.

B. Evolved Gas Analysis

Gas was sampled in the wake of pyrolyzing samples of M30, HMX and developmental RDX/HTPB binder propellant. Sampling probe position was typically 5 mm downstream and centered on the sample. Nitrogen flows at less than 1 m/s with temperatures of 310 to 580°C were used to obtain rapid pyrolysis without any visible flame. Under these conditions a sample would typically heat for a few seconds with no visible reactions and then fizz burn in the flow for up to several seconds. Figure 4 shows a typical infrared absorption spectrum from M30 pyrolysis. As can be seen in the figure, there are no major unassigned peaks. As the sample was configured, the gases taken should be dominated by gases from the exterior (front) surface and have minor input from perforation generated gases.

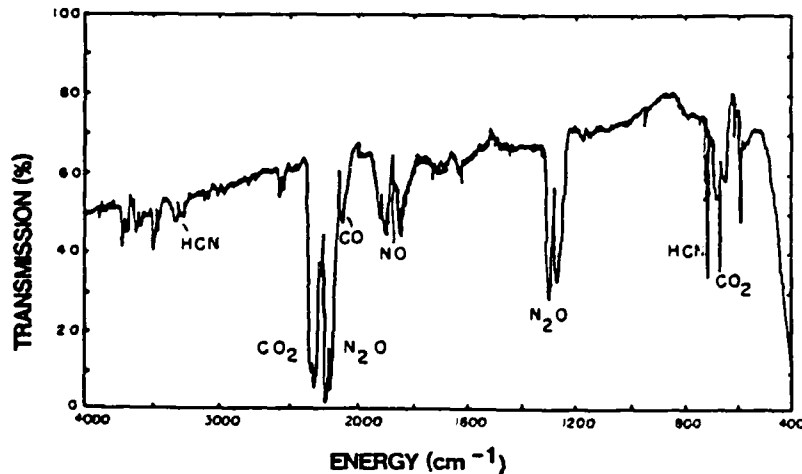


Figure 4. Infrared Absorption Spectrum of Gases Collected in the Wake of M30 Propellant Grain Pyrolyzed by Flow of 390°C Nitrogen

The HMX and RDX-binder samples yielded similar spectra under these conditions. With the binder, the RDX was stripped from the grain leaving a carcass of partially decomposed binder which was recognizable as a propellant grain with some aerodynamic modification. Spectra from lower and higher temperature pyrolysis of HMX pellets are shown in Figure 5. The main distinguishing features are the large quantities of NO₂ (vs. NO with M30), reduced amounts of CO₂, and additional peaks at the higher temperature.

It was found after these and similar spectra were taken that the small amount of room air in the sampling tube was affecting the NO/NO₂ balance. Because of equipment problems, it was not feasible to repeat the HMX pellet experiments. However, for the RDX/HTPB pyrolysis series, a slow purge flow of nitrogen was maintained in the non-evacuated portion of the sampling system until the time of sampling. A typical spectrum from this series is shown in Figure 6. It is clear in this figure that there are substantial amounts of NO present under these conditions. However, the NO₂ remains even under conditions where none can be seen from M30 pyrolysis.

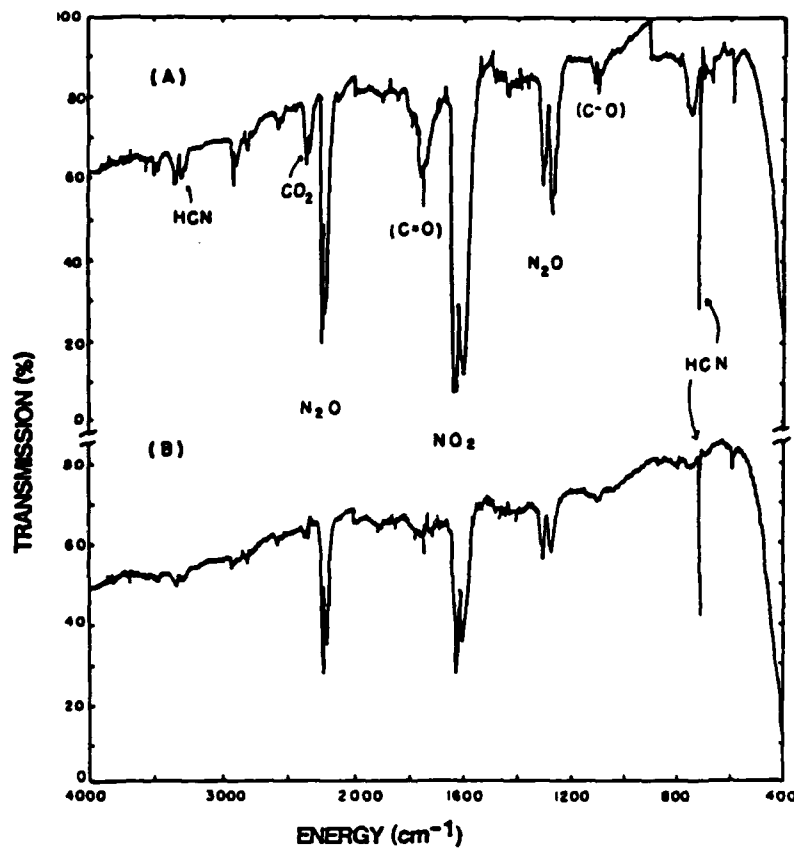


Figure 5. Infrared Absorption Spectrum of Gases Collected in the Wake of HMX Pellet Pyrolyzed by Flow of (a) 560°C and (b) 390°C Nitrogen

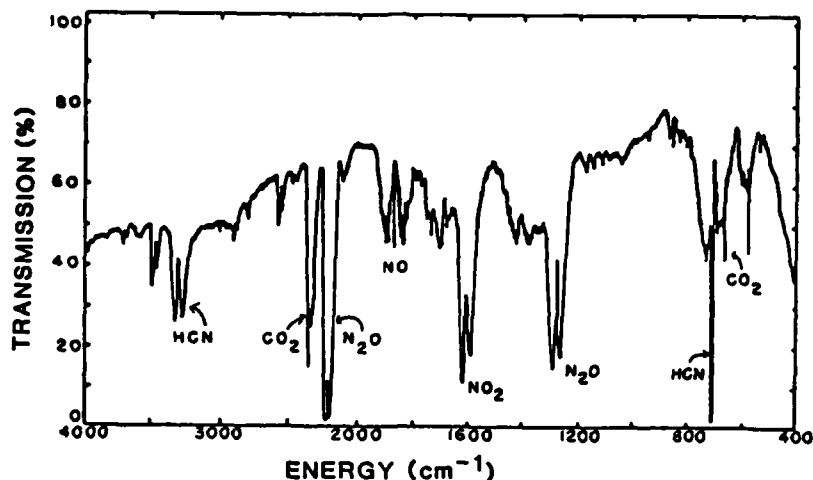


Figure 6. Infrared Absorption Spectrum of Gases From Pyrolysis of RDX/HTPB by 360°C Nitrogen

C. Planar Fluorescence

With the 35 mm camera setup, good signals were recorded at shutter speeds up to about 1/60 s. At faster shutter speeds, the NO₂ fluorescence is visible but weak in good quality prints made from the negatives. The high speed films shot at 400 frames/s through the 500 nm cut off filter showed weak fluorescence that is just visible when projected in a dark room. The level of signal is clearly not sufficient for even qualitative observations. As a test of the amount of increased light that might be needed to make useable films, a roll of film was exposed at 300 frames/s with the laser beam unexpanded and directed just downstream of the grain. In this case the bright green fluorescence of the NO₂ is clearly present as a line and readily distinguished from even the sodium emission when the pyrolysis gases are burning downstream of the laser beam. Thus it appears that the possibility of making useable films at 500 frames/s or faster requires only slight (on the order of factor of two) improvements in laser power or sensitivity of detection (e.g., image intensifiers). The additional usefulness of such high repetition rate lasers as the copper vapor laser is clearly possible if coincidences exist between their lines and molecules such as C₂ and, of course, NO₂.

IV. DISCUSSION/ANALYSIS

Several points can be learned from the emission and shadowgraph observations. The first is that with a flow of air (and presumably any other oxidizer-rich gas) ignition of the system begins in the wake and propagates back to the solid propellant. Whether this phenomenon also occurs in the case of inert flows is not clear from these observations. However, considering the gas products sampled in the pyrolysis of M30, it seems likely that these gases

would neither ignite as easily as with NO_2 present nor would they propagate with as great a flame velocity. Thus the air flow may well be re-oxidizing the NO to form NO_2 (for example) to provide gases which ignite and burn rapidly enough to produce the events as observed, or the oxygen may be participating directly in the ignition chemistry. If this is the case, one might expect nitramine propellants to exhibit much different behavior due to the greater reactivity of the gases evolved from them. However, our preliminary observations with RDX-binder grains suggests that these gases are released slowly enough that there is substantial dilution by the inert flowing gas; no attempts were made to ignite RDX pellets.

The full significance of the gas generation from grain perforations is not clear for M30, since the chemistry appears to be proceeding to a significant extent at the surface even though the inert heating gas should be diluting the evolved gases with convective flow. Under some conditions it is possible that more gas phase reactions might take place inside the perforations; no careful separation of the gases has been done on the basis of their origin (front surface vs. perforation).

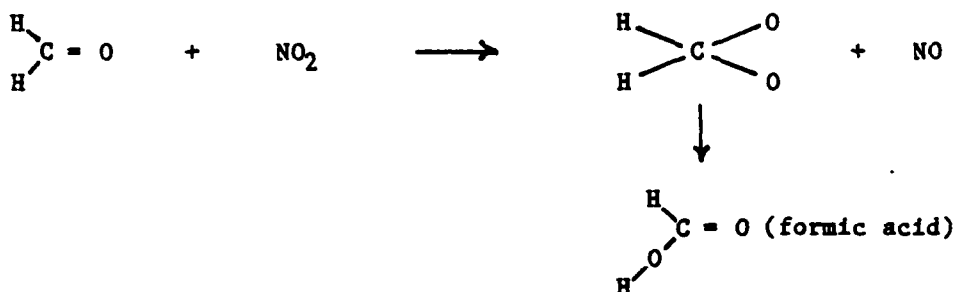
The implications of the large gas generation rate of the NOSOL propellant are not clear. The obvious breaking off of pieces of the grain throughout the sequence suggests that the observed phenomenon is merely a surface area effect; smaller particles may be generated at a substantial rate on the upstream side of the grain. Also of considerable interest with the NOSOL is the apparent development of a two-stage flame. A reasonable interpretation of the observed phenomenon is that the flame most distant from the grain (upstream) is a gas phase premixed flame of HCN , H_2CO , N_2O , NO , or other typical gases which might survive to that point. The area of heat release near the grain clearly extends sufficiently away from the surface to suggest a process beyond simple heat release at the surface of the grain. Because of the extent of this region, the most likely explanation once again appears to be that the observed heat release is the exothermic decomposition and reaction of a cloud of small propellant particles which are moving away from the surface. It does not appear likely that a mechanism of deconsolidation on the scale of that of pressed HMX under some conditions³ is operating here due to the differences in the physical makeup of the propellants. Whether this effect may be related to the nature of these particular experiments is not clear. The M30 samples, which have similar burning rates and impetus, show no similar effects. It is unlikely that this limited grain deconsolidation would be very apparent in a standard strand burner at elevated pressure; persons with extensive experience with this propellant in strand burners have noticed no unusual behavior and certainly nothing suggesting deconsolidation on a scale similar to that of pressed HMX .

As noted above there is a considerable difference in the gas phase products noted for M30 and the nitramines. In particular, it is quite clear that the reactions have progressed to a greater extent at or near the surface of the double base propellant. Supporting this conclusion are the relative

³R.A. Fifer and J.E. Cole, "Burning Rate for Steel-Cased, Pressed Binderless HMX ," Proceedings of the 17th JANNAF Combustion Meeting, CPIA Publication No. 329, Vol. II, p. 413, 1980.

amount of NO_2 and NO (even after correction of air contamination), and the appearance of CO , CO_2 and H_2O as reaction products. Our earlier low pressure studies indicate that the principal reactant with NO_2 is formaldehyde (HCHO), which is likely present but would not be readily detected by this sampling technique. For all pyrolysis cases here, the major gas phase products appear to be virtually the same as reported in our earlier studies⁴ of heating with hot filaments or by laser radiation. Thus there appears to be no decrease in surface or near surface reactions due to a dilution or transport effect of the pyrolyzing gas under the conditions of these observations.

Of note in the two HMX spectra is the increase in the two peaks near 1100 cm^{-1} and 1750 cm^{-1} as the temperature of the pyrolyzing gas increases. Comparison with spectra recorded on various neat gases suggests that these are the $\text{C}=\text{O}$ and $\text{C}-\text{O}$ vibrations of formic acid (H_2CO_2). This would be an intermediate product in the oxidation of formaldehyde by NO_2 via the following scheme:



Such a scheme is analogous to $\text{O} + \text{H}_2\text{CO}$ reaction pathways previously proposed by Chang and Barker.⁵ In the present case the formic acid could be formed in the ground electronic state and probably with sufficiently low excess energy to allow collisional stabilization. Because the formic acid would normally be consumed in any reaction or flame going to equilibrium, this observation may demonstrate the presence of an important reaction intermediate using a relatively unsophisticated experimental technique. The gas flow temperature here, in excess of 500°C cannot be duplicated in conventional pyrolysis at atmospheric pressure without the reaction approaching completion. Of course, the possibility that the formic acid is formed during sampling has not been discounted. It is considered unlikely that it is related to any contamination of the samples. It appears in other samples, although not always as well defined as in those spectra shown in Figure 5.

⁴R.A. Beyer, "Molecular Beam Sampling Mass Spectroscopy of High Heating Rate Pyrolysis," ARBRL-MR-02816, 1978 (A054328).

⁵J.S. Chang and J.R. Barker, "Reaction Rate and Products for the Reaction $\text{O}(^3\text{P}) + \text{H}_2\text{CO}$," J. Phys. Chem., Vol. 33, p. 3059, 1979.

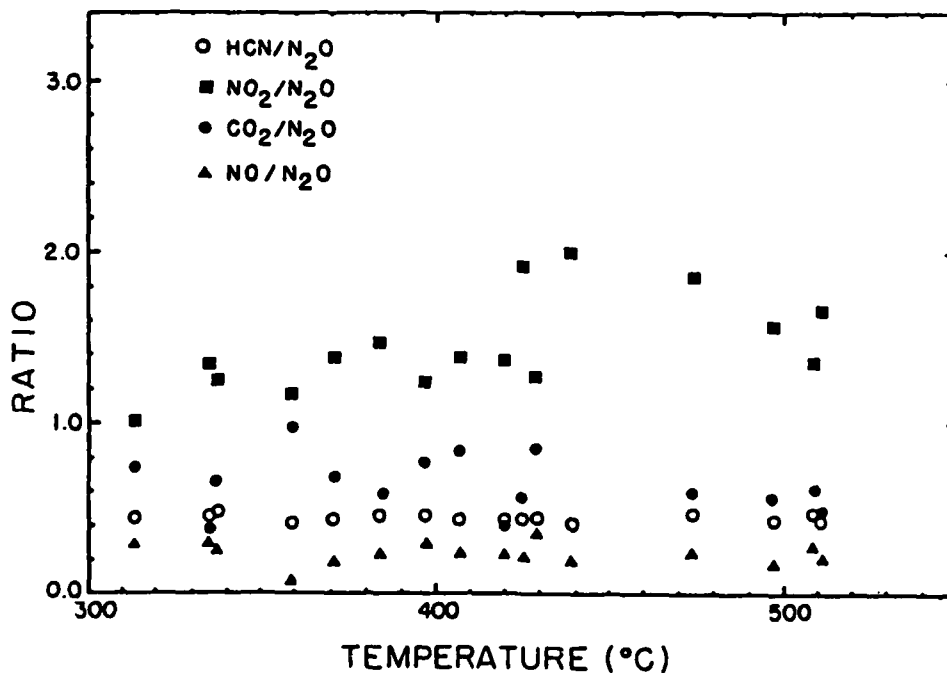


Figure 7. The Ratios of Four Major Species to N₂O at a Constant Flow Velocity Near 1 m/s as a Function of the Nitrogen Temperature at the Position of the Grain

A plot of the ratios of the five readily identifiable major species observed in the pyrolysis of RDX/HTPB is shown in Figure 7 as a function of temperature. Although the data are somewhat noisy, several trends appear to be present. Three of the species, HCN, NO, and CO₂, appear to be constant with respect to N₂O as the temperature is increased. Although the trend is not dramatic, the NO₂/N₂O ratio appears to increase as the temperature of the pyrolyzing gas increases. A possible interpretation of these observations is that the decomposition mechanism is changing as a function of temperature. However, it appears to be equally likely that the change in NO₂ may be due to the more rapid breakdown of the binder matrix, allowing this highly reactive gas to escape further reactions more readily at the higher temperatures. Hence it is probably not wise to draw conclusions about decomposition mechanisms before measurements are completed on pressed samples of pure RDX and HMX.

SUMMARY

The major observations and conclusions of this study are the following:

Ignition in the wake of a double base propellant grain is common when a flow of air is used at 1 m/s.

The apparent gas generation rate near the surface for NOSOL 363 is much greater than M30 under these conditions; this may indicate small scale deconsolidation of NOSOL.

NOSOL 363 propellant grains have a much greater tendency than M30 to break off chunks which burn downstream in a convective flow even at flows of 1 m/s.

The infrared analysis of convective pyrolysis products for M30 and BMK are similar to those produced by more conventional heating in earlier experiments.

The reactivity of gases evolved from RDX is much greater than those from double base propellants under these conditions.

Planar laser induced fluorescence of NO_2 should provide sufficient signal levels for diagnostics of nitramine propellant ignition at rates up to 500 frames/s with commercially available cw argon ion lasers.

ACKNOWLEDGEMENTS

The authors gratefully acknowledge the assistance of Dr. Nathan Klein in providing the equipment and expertise for the shadowgraph recording, Mr. Wade Scott for assistance with data acquisition, and Mr. Roger Bowman for key discussions and for providing some of the samples used. The comments of Richard Field, LCWSL, Dover, NJ, who reviewed the shadowgraph films of NOSOL 363 ignition, were invaluable.

REFERENCES

1. T.C. Minor, "Characterization of Ignition Systems for Bagged Artillery Charges," Proceedings of 17th JANNAF Combustion Meeting, CPIA Publication No. 329, Vol. II, p. 45, 1980.
2. S.E. Mitchell, "Selected Properties of Navy Gun Propellants," IHSP, pp. 76-128, 1976.
3. R.A. Fifer and J.E. Cole, "Burning Rate for Steel-Cased, Pressed Binderless HMX," Proceedings of the 17th JANNAF Combustion Meeting, CPIA Publication No. 329, Vol. II, p. 413, 1980.
4. R.A. Beyer, "Molecular Beam Sampling Mass Spectroscopy of High Heating Rate Pyrolysis," ARBRL-MR-02816, 1978 (A054328).
5. J.S. Chang and J.R. Barker, "Reaction Rate and Products for the Reaction $O(^3P) + H_2CO$," J. Phys. Chem., Vol. 33, p. 3059, 1959.

DISTRIBUTION LIST

<u>No. Of Copies</u>	<u>Organization</u>	<u>No. Of Copies</u>	<u>Organization</u>
12	Administrator Defense Technical Info Center ATTN: DTIC-DDA Cameron Station Alexandria, VA 22304-6145	1	Director USA Air Mobility Research and Development Laboratory Ames Research Center Moffett Field, CA 94035
1	HQ DA DAMA-ART-M Washington, DC 20310	4	Commander US Army Research Office ATTN: R. Ghirardelli D. Mann R. Singleton R. Shaw Research Triangle Park, NC 27709
1	Commander U.S. Army Materiel Command ATTN: AMCDRA-ST 5001 Eisenhower Avenue Alexandria, VA 22333-0001	1	Commander USA Communications - Electronics Command ATTN: AMSEL-ED Fort Monmouth, NJ 07703
1	Commander Armament R&D Center USA AMCCOM ATTN: SMCAR-TSS Dover, NJ 07801	1	Commander USA Electronics Research and Development Command Technical Support Activity ATTN: DELSD-L Fort Monmouth, NJ 07703-5301
2	Commander Armament R&D Center USA AMCCOM ATTN: SMCAR-TDC Dover, NJ 07801	2	Commander USA AMCCOM ATTN: SMCAR-LCA-G, D.S. Downs J.A. Lannon Dover, NJ 07801
1	Director Benet Weapons Laboratory Armament R&D Center USA AMCCOM ATTN: SMCAR-LCB-TL Watervliet, NY 12189	1	Commander USA AMCCOM ATTN: SMCAR-LC-G, L. Harris Dover, NJ 07801
1	Commander USA Army Armament, Munitions and Chemical Command ATTN: SMCAR-ESP-L Rock Island, IL 61299	1	Commander USA AMCCOM ATTN: SMCAR-SCA-T, L. Stiefel Dover, NJ 07801



DISTRIBUTION LIST

<u>No. Of Copies</u>	<u>Organization</u>	<u>No. Of Copies</u>	<u>Organization</u>
1	University of Michigan Gas Dynamics Laboratory Aerospace Engineering Bldg. ATTN: G. M. Faeth Ann Arbor, MI 48109-2140	1	Commander Naval Air Systems Command ATTN: J. Ramnarace, AIR-54111C Washington, DC 20360
2	Commander USA Missile Command ATTN: AMSMI-RK, D.J. Ifshin W. Wharton Redstone Arsenal, AL 35898	1	Commander Naval Surface Weapons Center ATTN: J.L. East, Jr., G-23 Dahlgren, VA 22448
1	Commander USA Tank Automotive Command ATTN: AMSTA-TSL Warren, MI 48090	2	Commander Naval Surface Weapons Center ATTN: R. Bernecker, R-13 G.B. Wilmot, R-16 Silver Spring, MD 20910
1	Director USA TRADOC Systems Analysis Activity ATTN: ATAA-SL WSMR, NM 88002	4	Commander Naval Weapons Center ATTN: R.L. Derr, Code 389 China Lake, CA 93555
2	Commandant US Army Infantry School ATTN: ATSH-CD-CSO-OR Fort Benning, GA 31905	2	Commander Naval Weapons Center ATTN: Code 3891, T. Boggs K.J. Graham China Lake, CA 93555
1	Commander USA Army Development and Employment Agency ATTN: MODE-TED-SAB Fort Lewis, WA 98433	5	Commander Naval Research Laboratory ATTN: L. Harvey J. McDonald E. Oran J. Shnur R.J. Doyle, Code 6110 Washington, DC 20375
1	Office of Naval Research Department of the Navy ATTN: R.S. Miller, Code 432 800 N. Quincy Street Arlington, VA 22217	1	Commanding Officer Naval Underwater Systems Center Weapons Dept. ATTN: R.S. Lazar/Code 36301 Newport, RI 02840

DISTRIBUTION LIST

<u>No. Of Copies</u>	<u>Organization</u>	<u>No. Of Copies</u>	<u>Organization</u>
1	Superintendent Naval Postgraduate School Dept. of Aeronautics ATTN: D.W. Netzer Monterey, CA 93940	1	Applied Combustion Technology, Inc. ATTN: A.M. Varney P.O. Box 17885 Orlando, FL 32860
6	AFRPL (DRSC) ATTN: R. Geisler D. George B. Goshgarian J. Levine W. Roe D. Weaver Edwards AFB, CA 93523-5000	2	Applied Mechanics Reviews The American Society of Mechanical Engineers ATTN: R.E. White A.B. Wenzel 345 E. 47th Street New York, NY 10017
2	AFOSR ATTN: L.H. Caveny J.M. Tishkoff Bolling Air Force Base Washington, DC 20332	2	Atlantic Research Corp. ATTN: M.K. King 5390 Cherokee Avenue Alexandria, VA 22314
1	AFWL/SUL Kirtland AFB, NM 87117	1	Atlantic Research Corp. ATTN: R.H.W. Waesche 7511 Wellington Road Gainesville, VA 22065
1	Air Force Armament Laboratory ATTN: AFATL/DLODL Eglin AFB, FL 32542-5000	1	AVCO Everett Rsch. Lab. Div. ATTN: D. Stickler 2385 Revere Beach Parkway Everett, MA 02149
1	NASA Langley Research Center ATTN: G.B. Northam/MS 168 Hampton, VA 23365	1	Battelle Memorial Institute Tactical Technology Center ATTN: J. Huggins 505 King Avenue Columbus, OH 43201
4	National Bureau of Standards ATTN: J. Hastie M. Jacox T. Kashiwagi H. Semerjian US Department of Commerce Washington, DC 20234	2	Exxon Research & Eng. Co. ATTN: A. Dean M. Chou P.O. Box 45 Linden, NJ 07036
1	Aerojet Solid Propulsion Co. ATTN: P. Micheli Sacramento, CA 95813	1	Ford Aerospace and Communications Corp. DIVAD Division Div. Hq., Irvine ATTN: D. Williams Main Street & Ford Road Newport Beach, CA 92663

DISTRIBUTION LIST

<u>No. Of Copies</u>	<u>Organization</u>	<u>No. Of Copies</u>	<u>Organization</u>
1	General Electric Armament & Electrical Systems ATTN: M.J. Bulman Lakeside Avenue Burlington, VT 05402	1	IBM Corporation ATTN: A.C. Tam Research Division 5600 Cottle Road San Jose, CA 95193
1	General Electric Company ATTN: Alan Wait Rd 3, Plains Rd Ballston Spa, NY 12020	2	Director Lawrence Livermore National Laboratory ATTN: C. Westbrook M. Costantino P.O. Box 808 Livermore, CA 94550
1	General Electric Ordnance Systems ATTN: J. Mandzy 100 Plastics Avenue Pittsfield, MA 01203	1	Lockheed Missiles & Space Co. ATTN: George Lo 3251 Hanover Street Dept. 52-35/B204/2 Palo Alto, CA 94304
1	General Motors Rsch Labs Physics Department ATTN: R. Teets Warren, MI 48090	1	Los Alamos National Lab ATTN: B. Nichols T7, MS-B284 P.O. Box 1663 Los Alamos, NM 87545
3	Hercules, Inc. Alleghany Ballistics Lab. ATTN: R.R. Miller P.O. Box 210 Cumberland, MD 21501	1	Olin Corporation Smokeless Powder Operations P.O. Box 222 St. Marks, FL 32355
3	Hercules, Inc. Bacchus Works ATTN: K.P. McCarty P.O. Box 98 Magna, UT 84044	1	Paul Gough Associates, Inc. ATTN: P.S. Gough 1048 South Street Portsmouth, NH 03801
1	Honeywell, Inc. Defense Systems Division ATTN: D. E. Broden/ MS MN50-2000 600 2nd Street NE Hopkins, MN 55343	2	Princeton Combustion Research Laboratories, Inc. ATTN: M. Summerfield N.A. Messina 475 US Highway One Monmouth Junction, NJ 08852
		1	Hughes Aircraft Company ATTN: T.E. Ward 8433 Fallbrook Avenue Canoga Park, CA 91303

DISTRIBUTION LIST

<u>No. Of Copies</u>	<u>Organization</u>	<u>No. Of Copies</u>	<u>Organization</u>
1	Rockwell International Corp. Rocketdyne Division ATTN: J.E. Flanagan/HBO2 6633 Canoga Avenue Canoga Park, CA 91304	1	Thiokol Corporation Elkton Division ATTN: W.N. Brundige P.O. Box 241 Elkton, MD 21921
3	Sandia National Laboratories Combustion Sciences Dept. ATTN: R. Cattolica D. Stephenson P. Mattern Livermore, CA 94550	3	Thiokol Corporation Huntsville Division ATTN: R. Glick Huntsville, AL 35807
1	Sandia National Laboratories Division 8353 Livermore, CA 94550	1	Thiokol Corporation Wasatch Division P.O. Box 524 Brigham City, UT 84302
1	Science Applications, Inc. ATTN: R.B. Edelman 23146 Cumorah Crest Woodland Hills, CA 91364	1	United Technologies ATTN: A.C. Eckbreth East Hartford, CT 06108
1	Science Applications, Inc. ATTN: H.S. Pergament 1100 State Road, Bldg. N Princeton, NJ 08540	2	United Technologies Corp. ATTN: R.S. Brown R.O. McLaren P.O. Box 358 Sunnyvale, CA 94088
4	SRI International ATTN: G. Smith D. Crosley D. Golden 333 Ravenswood Avenue Menlo Park, CA 94025	1	Universal Propulsion Company ATTN: H.J. McSpadden Black Canyon Stage 1 Box 1140 Phoenix, AZ 85029
1	Stevens Institute of Tech. Davidson Laboratory ATTN: R. McAlevy, III Hoboken, NJ 07030	1	Veritay Technology, Inc. ATTN: E.B. Fisher 4845 Millersport Highway P.O. Box 305 East Amherst, NY 14051-0505
1	Teledyne McCormack-Selph ATTN: C. Leveritt 3601 Union Road Hollister, CA 95023	1	Brigham Young University Dept. of Chemical Engineering ATTN: M.W. Beckstead Provo, UT 84601
		1	California Institute of Tech. Jet Propulsion Laboratory ATTN: MS 125/159 4800 Oak Grove Drive Pasadena, CA 91103

DISTRIBUTION LIST

<u>No. Of Copies</u>	<u>Organization</u>	<u>No. Of Copies</u>	<u>Organization</u>
1	California Institute of Technology ATTN: F.E.C. Culick/ MC 301-46 204 Karman Lab. Pasadena, CA 91125	1	University of Florida Dept. of Chemistry ATTN: J. Winefordner Gainesville, FL 32611
1	University of California, Berkeley Mechanical Engineering Dept. ATTN: J. Daily Berkeley, CA 94720	3	Georgia Institute of Technology School of Aerospace Engineering ATTN: E. Price W.C. Strahle B.T. Zinn Atlanta, GA 30332
1	University of California Los Alamos National Lab. ATTN: T.D. Butler P.O. Box 1663, Mail Stop B216 Los Alamos, NM 87545	1	University of Illinois Dept. of Mech. Eng. ATTN: H. Krier 144MEB, 1206 W. Green St. Urbana, IL 61801
2	University of California, Santa Barbara Quantum Institute ATTN: K. Schofield M. Steinberg Santa Barbara, CA 93106	1	Johns Hopkins University/APL Chemical Propulsion Information Agency ATTN: T.W. Christian Johns Hopkins Road Laurel, MD 20707
1	University of Southern California Dept. of Chemistry ATTN: S. Benson Los Angeles, CA 90007	1	University of Minnesota Dept. of Mechanical Engineering ATTN: E. Fletcher Minneapolis, MN 55455
1	Case Western Reserve Univ. Div. of Aerospace Sciences ATTN: J. Tien Cleveland, OH 44135	4	Pennsylvania State University Applied Research Laboratory ATTN: K. K. Kuo H. Palmer M. Micci University Park, PA 16802
1	Cornell University Department of Chemistry ATTN: E. Grant Baker Laboratory Ithaca, NY 14853	1	Polytechnic Institute of NY ATTN: S. Lederman Route 110 Farmingdale, NY 11735
1	Univ. of Dayton Rsch Inst. ATTN: D. Campbell AFRPL/PAP Stop 24 Edwards AFB, CA 93523		

DISTRIBUTION LIST

<u>No. Of Copies</u>	<u>Organization</u>	<u>No. Of Copies</u>	<u>Organization</u>
2	Princeton University Forrestal Campus Library ATTN: K. Brezinsky I. Glassman P.O. Box 710 Princeton, NJ 08540	1	Virginia Polytechnic Institute and State University ATTN: J.A. Schetz Blacksburg, VA 24061
			<u>Aberdeen Proving Ground</u>
1	Princeton University MAE Dept. ATTN: F.A. Williams Princeton, NJ 08544		Dir, USAMSAA ATTN: AMXSY-D AMXSY-MP, H. Cohen
1	Purdue University School of Aeronautics and Astronautics ATTN: J.R. Osborn Grissom Hall West Lafayette, IN 47907		Cdr, USATECOM ATTN: AMSTE-TO-F Cdr, CRDC, AMCCOM ATTN: SMCCR-RSP-A SMCCR-MU SMCCR-SPS-IL
2	Purdue University School of Mechanical Engineering ATTN: N.M. Laurendeau S.N.B. Murthy TSPC Chaffee Hall West Lafayette, IN 47906		
1	Rensselaer Polytechnic Inst. Dept. of Chemical Engineering ATTN: A. Fontijn Troy, NY 12181		
1	Stanford University Dept. of Mechanical Engineering ATTN: R. Hanson Stanford, CA 93106		
1	University of Texas Dept. of Chemistry ATTN: W. Gardiner Austin, TX 78712		
1	University of Utah Dept. of Chemical Engineering ATTN: G. Flandro Salt Lake City, UT 84112		

USER EVALUATION SHEET/CHANGE OF ADDRESS

This Laboratory undertakes a continuing effort to improve the quality of the reports it publishes. Your comments/answers to the items/questions below will aid us in our efforts.

1. BRL Report Number _____ Date of Report _____
2. Date Report Received _____
3. Does this report satisfy a need? (Comment on purpose, related project, or other area of interest for which the report will be used.) _____

4. How specifically, is the report being used? (Information source, design data, procedure, source of ideas, etc.) _____

5. Has the information in this report led to any quantitative savings as far as man-hours or dollars saved, operating costs avoided or efficiencies achieved, etc? If so, please elaborate. _____

6. General Comments. What do you think should be changed to improve future reports? (Indicate changes to organization, technical content, format, etc.) _____

CURRENT ADDRESS

Name

Organization

Address

City, State, Zip

7. If indicating a Change of Address or Address Correction, please provide the New or Correct Address in Block 6 above and the Old or Incorrect address below.

OLD ADDRESS

Name

Organization

Address

City, State, Zip

(Remove this sheet along the perforation, fold as indicated, staple or tape closed, and mail.)

FOLD HERE

Director
U.S. Army Ballistic Research Laboratory
ATTN: SLCBR-DD-T
Aberdeen Proving Ground, MD 21005-5066



NO POSTAGE
NECESSARY
IF MAILED
IN THE
UNITED STATES

OFFICIAL BUSINESS
PENALTY FOR PRIVATE USE. \$300

BUSINESS REPLY MAIL
FIRST CLASS PERMIT NO 12062 WASHINGTON, DC
POSTAGE WILL BE PAID BY DEPARTMENT OF THE ARMY



Director
U.S. Army Ballistic Research Laboratory
ATTN: SLCBR-DD-T
Aberdeen Proving Ground, MD 21005-9989

FOLD HERE

END

FILMED

3-86

DTIC